

Semi-empirical model for indirect measurement of soot size distributions in compression ignition engines

Francisco, Martos; Martin-Gonzalez, Gema; Herreros, Jose

DOI:

[10.1016/j.measurement.2018.03.081](https://doi.org/10.1016/j.measurement.2018.03.081)

License:

Creative Commons: Attribution-NonCommercial-NoDerivs (CC BY-NC-ND)

Document Version

Peer reviewed version

Citation for published version (Harvard):

Francisco, M, Martin-Gonzalez, G & Herreros, J 2018, 'Semi-empirical model for indirect measurement of soot size distributions in compression ignition engines', *Measurement*, vol. 124, pp. 32-39.
<https://doi.org/10.1016/j.measurement.2018.03.081>

[Link to publication on Research at Birmingham portal](#)

Publisher Rights Statement:

Checked for eligibility: 11/04/2018

General rights

Unless a licence is specified above, all rights (including copyright and moral rights) in this document are retained by the authors and/or the copyright holders. The express permission of the copyright holder must be obtained for any use of this material other than for purposes permitted by law.

- Users may freely distribute the URL that is used to identify this publication.
- Users may download and/or print one copy of the publication from the University of Birmingham research portal for the purpose of private study or non-commercial research.
- User may use extracts from the document in line with the concept of 'fair dealing' under the Copyright, Designs and Patents Act 1988 (?)
- Users may not further distribute the material nor use it for the purposes of commercial gain.

Where a licence is displayed above, please note the terms and conditions of the licence govern your use of this document.

When citing, please reference the published version.

Take down policy

While the University of Birmingham exercises care and attention in making items available there are rare occasions when an item has been uploaded in error or has been deemed to be commercially or otherwise sensitive.

If you believe that this is the case for this document, please contact UBIRA@lists.bham.ac.uk providing details and we will remove access to the work immediately and investigate.

Semi-empirical model for indirect measurement of soot size distributions in compression ignition engines

Martos, F.J.,^{a,*}, Martín-González, G.^a, Herreros, J.M.^b

^a*Escuela de Ingenierías Industriales, University of Málaga, c/Doctor Ortiz Ramos, s/n, 29071, Málaga, Spain*

^b*School of Mechanical Engineering, University of Birmingham, Edgbaston, B15 2TT, UK*

Abstract

1 This work proposes a semi-empirical model, which provides soot particle
2 size distribution functions emitted by compression ignition engines. The model
3 is composed of a phenomenological model based on the collision dynamics of
4 particle agglomerates and an empirical model, which provides key input pa-
5 rameters such as primary particle size and a mathematical relationship between
6 the size of the agglomerate and number of primary particles. The phenom-
7 logical model considers the relevant fluid-dynamics phenomena influencing the
8 collision frequency function. It is observed that Brownian motion is the pre-
9 dominant phenomenon and in a much lesser degree inertial turbulent motion.
10 The experimental model requires air/fuel ratio, engine speed, soot density and
11 mean instantaneous in-cylinder pressure. A Dirac delta is used as a seed for the
12 agglomerate size function whose magnitude depends on the soot volume concen-
13 tration and the mean primary particle size at each engine operation condition.
14 In a further step, the obtained modelled agglomerate size functions are fitted
15 to lognormal size distributions defined by the modelled mean size and stan-
16 dard deviation. Modelled lognormal agglomerate size distribution functions are
17 validated with respect to experimental distributions obtained using a Scanning
18 Mobility Particle Sizer (SMPS).

Keywords: particle size distribution function, soot, compression ignition engines, semi-empirical modelling

*Corresponding author

Email address: fjmartos@uma.es (Martos, F.J.,)
Preprint submitted to Measurement

19 1. Introduction

20 Compression ignition engines have significant advantages in terms of engine
21 performance, fuel economy and CO₂ emissions compared to spark ignition en-
22 gines. However, they have the drawback of high NO_x and particulate matter
23 (PM) emissions derived from their non-homogeneous combustion process. Reg-
24 ulatory actions aiming to mitigate the environmental [1] and public health [2]
25 effects of particulate matter released by vehicles have been put in place. The
26 mass of PM emissions has been regulated in Europe since Euro 1 in light duty
27 passenger cars and commercial vehicles powered by diesel engines. Particle
28 size affects (i) particle reactivity through the surface/volume ratio, (ii) parti-
29 cle suspension time in the atmosphere and (iii) particle trapping efficiency in
30 a filtration system, and thus the environmental and health effects of particles.
31 As a result, since the entry into force in Europe of Euro 5b in September 2011
32 [3], not only the mass emissions of particles are regulated but also the total
33 number of particles for both diesel and gasoline powered vehicles. It could be
34 also evaluated the possibility to introduce the particle size as a limitation factor
35 in the future.

36 Particles are formed in locally rich-in-fuel regions in the combustion cham-
37 ber. Fuel molecules which do not have access to oxygen are pyrolysed producing
38 aromatics and other hydrocarbon species (such as C₂H₂, C₂H₄, C₃H₆, C₄H₄),
39 which can act as polycyclic aromatic hydrocarbons (PAHs) and soot precursors.
40 PAHs from a certain size condense forming a 1-2 nm nuclei (nucleation). Those
41 nuclei undergoes surface growth maintaining a quasi-spherical shape [4, 5] while
42 increasing the C/H ratio forming the so-called primary particles with sizes be-
43 tween 15 and 30 nm depending on fuel, engine and engine operation condition.
44 Thereafter, particle agglomerates are formed as a consequence of collisions be-
45 tween the primary particles and/or primary particles and agglomerates. The
46 formed agglomerates loose the spherical shape becoming like-fractal structures
47 [6, 7], thus equivalent diameters based on different properties are defined to
48 quantify agglomerate size. Equivalent diameter of a non-spherical particle is

49 the diameter of a spherical particle that gives the same value of a specific prop-
50 erty (aerodynamic, electrical mobility, optical, etc.) to that of the non-spherical
51 agglomerate. For instance, electrical mobility diameter can be related by po-
52 tential functions with other characteristic sizes such as the radius of gyration
53 [8, 9].

54 The determination of particle size distribution functions not only provides
55 information related to the environmental and human health effects but also
56 could contribute to the diagnosis of the causes of particle formation as well as
57 to adopt actions for their abatement. Exhaust particle size distributions are
58 measured using particle sizer spectrometers such as Scanning Mobility Particle
59 Sizer (SMPS) [10], Engine Exhaust Particle Spectrometer (EEPS), Combustion
60 DMS 500 [11], Electrical Low Pressure Impactor (ELPI) [12], etc. These equip-
61 ment require the dilution of the exhaust to reproduce atmospheric conditions
62 and adapt the sample in temperature and particle concentration to be measured
63 by the equipment. Thus, this process could provoke quantitative and qualitative
64 differences to the agglomerate size distribution [13]. The modeling of size distri-
65 bution functions has been studied in [14] for generic aerosols or in works as [15],
66 [16] and [17] for soot aerosols. The complex nature of pollutant formation and
67 oxidation in compression ignition engines [18] and [19] results in the utilisation
68 of different types of models and/or their combination including phenomenolog-
69 ical (physically motivated relations), empirical (measured data to identify the
70 relations) [20] and hybrid approaches combining physical and empirical relations
71 (semi-empirical models) [21]. Phenomenological and empirical approaches both
72 have appropriate characteristics but also present disadvantages. Phenomeno-
73 logical models predict qualitative trends but the physically motivated relations
74 are difficult to identify [22] and [23] and have limitations from error propagation
75 and computational time [24]. On the other hand, empirical models are computa-
76 tional efficient, fit accurately to quantitative measurement results and are simple
77 to handle, [25]. The major limitation of empirical models is the lack of reliable
78 extrapolation beyond the conditions where the model is fitted and that only the
79 parameters explicitly present in the model could be identified. Semi-empirical

80 models combine the capabilities of physical models providing reliable qualitative
81 trends enabling the model extrapolation with minimum number of constraints
82 and measurements required to adjust the model as well as the computational
83 efficiency of empirical models [21].

84 This paper aims to develop a new methodology to estimate the size distribu-
85 tion function of the soot agglomerates emitted from compression ignition engines
86 using a semi-empirical model composed of a phenomenological and empirical
87 model. The model is validated with respect to agglomerate size distribution ex-
88 perimentally measured using an SMPS in the same engine operation conditions.
89 Section 2 describes the proposed semi-empirical model including the hypothe-
90 ses, phenomenological dynamics of the collisions between agglomerates, and the
91 relations between agglomerate size and number of primary particles. The ex-
92 perimental facilities and techniques used to obtain the input of the model (e.g.
93 in-cylinder pressure, engine speed, Air/Fuel ratio, and volumetric soot concen-
94 tration) are presented in Section 3. The experimental particle size distributions
95 and model validation are developed in Section 4, while conclusions are presented
96 in Section 5.

97 **2. Methodology and experimental installation**

98 The proposed semi-empirical model provides particle size distributions for
99 different engine operation conditions requiring instantaneous in-cylinder pres-
100 sure, total volumetric soot concentration, engine speed and Air/Fuel ratio as in-
101 puts. The obtained particle size distributions are in the nanometric range. The
102 model is composed of a phenomenological model to describe particle collisions
103 in the combustion chamber, as well as empirical models which feed the phe-
104 nomenological model (see figure 1). Particularly, the empirical model provides
105 the relationship between the initial primary particle size and engine operation
106 condition (engine speed, Air/Fuel ratio) as well as the correlation between the
107 number of primary particles per agglomerate and agglomerate size. The resul-
108 tant agglomerate size distribution is fitted to a log-normal distribution function

109 maintaining the mode and standard deviation. The results of the semi-empirical
 110 model are validated with respect to experimental agglomerate size distributions
 111 measured using an SMPS in the same engine operation conditions.

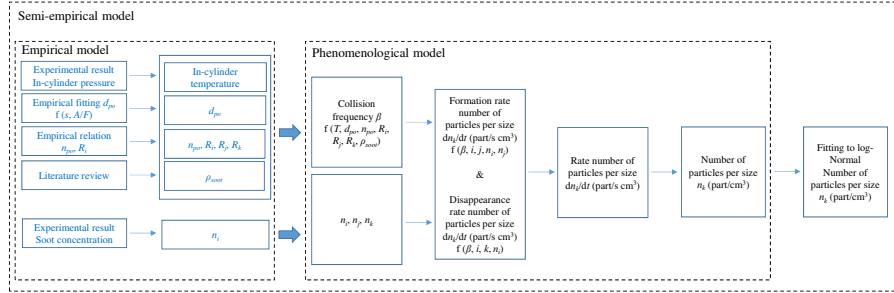


Figure 1: Scheme of the semi-empirical model

112 The experimental tests to obtain the required model input parameters and
 113 the results to validate the model have been carried out in a Nissan YD2.2
 114 turbocharged compression ignition engine operated by standard EN590 diesel
 115 fuel. An asynchronous brake, Schenck brand Dynas III LI 250 has been used
 116 to provide to the engine the desired operation load. Soot concentration pro-
 117 duced by the engine is measured with an AVL 415 smokemeter. The instan-
 118 tantaneous mean in-cylinder pressure values have been measured using a Kistler
 119 piezoelectric transducer model Z17090sp149. The crankshaft rotation angle has
 120 been measured with an optical angle encoder AVL364. These two signals have
 121 been synchronized by a Yokogawa OR1400 oscilloscope. From the instanta-
 122 neous mean in-cylinder pressure and by using a zero-dimensional thermody-
 123 namic model within the combustion chamber, [26, 27], the instantaneous mean
 124 temperature inside the combustion chamber can be obtained. A SMPS has been
 125 used to measure the particle size distribution function in the tailpipe to validate
 126 the semi-empirical model. The SMPS classifies the particles according to their
 127 mobility size. The SMPS used is from TSI, model 3936L10, and the particle
 128 counter is CPC model 3010S. The Differential Mobility Analyzer (DMA) has a
 129 sizing uncertainty of approximately 3 – 3.5%, [28]. The SMPS has a particle

130 size measurement range from 10 to 500 nm.

131 A reference engine operation condition extracted from the urban driving of
132 the light vehicle type-approval cycle has been chosen. This point has been de-
133 noted as L2. The engine load has been varied at this operating point, keeping
134 the rest of the engine’s operating parameters constant, such as the engine speed
135 maintained at 1525 rpm and EGR (0% EGR). The five engine test points are
136 summarised in the table 1, including torque, Air/Fuel ratio, brake mean ef-
137 fective pressure (BMEP) and the soot concentration, while the instantaneous
138 in-cylinder temperature is shown in Figure 2. The starting point for the model
139 has been located when the combustion starts in the combustion chamber, and
140 has been denoted as t_0 .

Operating mode	Torque (Nm)	Air/Fuel ratio	BMEP (bar)	C ($\text{mg}\cdot\text{m}^{-3}$)
L1	27.2	43.00	1.53	11.42
L2	45.4	32.28	2.63	16.25
L3	58.4	26.99	3.36	21.67
L4	70.8	23.37	4.08	62.20
L5	83.1	20.05	4.80	348.86

Table 1: Engine operating conditions.

141 3. Proposed model

142 The semi-empirical model solves the equations that express the balance of
143 the number of particles per size of a distribution function. The size distribution
144 is discretized in terms of the particle collision frequency to which is subjected an
145 initial mono-disperse population of primary particles under Brownian movement
146 [29].

147 3.1. Assumptions

- 148 1. Initially the aerosol is monodisperse. The aerosol considered at the begin-
149 ning of the simulation is monodisperse being composed of solid spherical

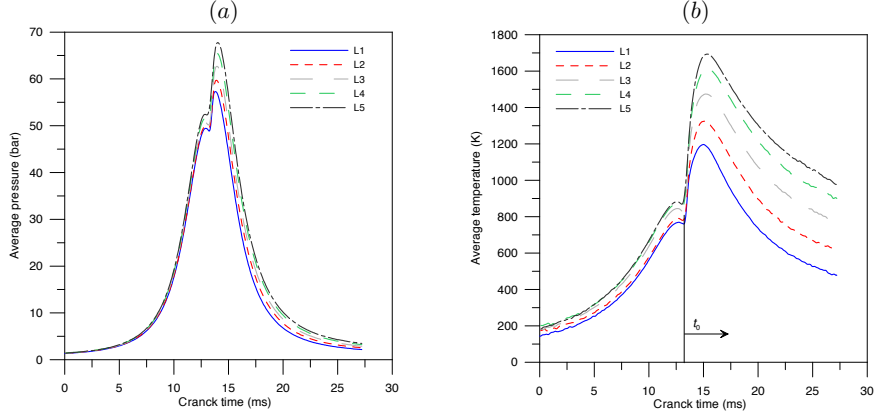


Figure 2: Average pressure (a) and average temperature (b) inside the combustion chamber vs. crank time.

- 150 primary particles in suspension, with a diameter d_{po} .
- 151 2. Conservation of mass. The mass of the particle formed after a collision is
 152 equal to the sum of the masses of the particles that collided.
- 153 3. Loss of identity of colliding particles. The particle formed after a collision
 154 of two particles has different fractal dimension to its progenitors, [30].
- 155 4. Instantaneous internal coalescence time. The collision and recombination
 156 processes to form the new particle is instantaneous.

157 *3.2. Collision dynamics of particle agglomerates*

158 The particle number concentration at size k (n_k) is obtained as the balance
 159 between the formation of new particles and the disappearance of particles of
 160 size k . Both of them are dependent from the number of particle collisions (N).
 161 The number of collisions between particles at size i and j can be calculated
 162 considering the frequency of particle collision (β_{ij}) and the concentration of
 163 particles at size i and j being mathematically expressed in equation (1).

$$N_{ij} = \beta(i, j) n_i n_j, \quad (1)$$

164 where $\beta(i, j)$ is the function of the collision frequency that depends on the size
 165 of the colliding particles and the gas properties (see further mathematical details
 166 in reference [31]), while n_i and n_j are the concentration of particles of size i and
 167 j per unit of volume.

168 Taking into consideration equation (1), the net rate of particles (forma-
 169 tion/disappearance) per particle size k at a given instant can be calculated (2).
 170 Therefore, the number of particles per particle size (agglomerate size distribu-
 171 tion) leaving the engine combustion chamber could be obtained from integration
 172 of Equation (2) assuming mass conservation and instantaneous internal coales-
 173 cence time. It has to be noted that the particle formation rate for size k ,
 174 ($k = i + j$), must be affected by a factor of $\frac{1}{2}$ in order to avoid duplication in
 175 formation.

$$\frac{dn_k}{dt} = \frac{1}{2} \sum_{i+j=k} \beta(i, j) n_i n_j - n_k \sum_{i=1}^{\infty} \beta(i, k) n_i \quad (2)$$

176 As commented above, the collision frequency function $\beta(i, j)$ depends on
 177 the number and characteristics of the particles involved in such collisions and
 178 the gas properties. Basically, there are two main mechanisms into a combustion
 179 chamber to drive the collisions: Brownian movement and inertial movement
 180 due to fluid turbulence. In the case under study, the inertial movement can
 181 be neglected in a first approximation. To show that, it is known that the
 182 characteristic scale of a soot agglomerate is $d_p \sim 100$ nm, [30]. On the other
 183 hand, at the Kolmogorov scale η viscosity dominates and the turbulent kinetic
 184 energy is dissipated into heat, being negligible the inertial movement. In other
 185 words, η is a measure of the size of eddies at which molecular viscosity becomes
 186 dominant. An estimate for the ratio of the largest L to smallest η length scales
 187 in turbulent flows is given in equation (3), [32].

$$\frac{L}{\eta} \sim \left(\frac{UL}{\nu} \right)^{3/4} = Re^{3/4}, \quad (3)$$

where Re , is the Reynolds number based on the large scale flow features, U is
 a characteristic velocity and L is a characteristic length, and ν , the kinematic

viscosity of the gas. For the engine under study, we can choose: as characteristic length the diameter of the cylinder $L \sim D = 86.5 \times 10^{-3}$ m; as characteristic velocity the mean piston speed, $U = 2 \times stroke \times n/60$, that for $n = 1525$ rpm and $stroke = 94 \times 10^{-3}$ m it is found $U = 4.78$ m/s; finally, for an average temperature inside the chamber of 1500 K and a pressure of 70 bar, the kinematic viscosity of the air is $\nu \sim 3.5 \times 10^{-6} m^2/s$. Thus, the Reynolds number for the large scales is $Re \sim 1.2 \times 10^5$. Therefore, Eq. 3 yields,

$$\eta \sim \frac{L}{Re^{3/4}} \sim 13.6 \times 10^{-6} \text{ m} = 13.6 \mu\text{m}, \quad (4)$$

188 which is the typical value for the Kolmogorov scale found in other studies [33]. In
 189 summary, since $\eta/d_p \sim 140$, the inertial movement can be neglected versus the
 190 Brownian movement in the collision frequency function $\beta(i, j)$ for soot particles.

191 As collision frequency is dominated by Brownian motion and the aerosol
 192 could be considered discreet (Knudsen number greater than 10), the function of
 193 collision frequency is obtained from the kinetic theory of gases, [31] and [34].

$$\beta(i, j) = \left(\frac{3\pi KT}{\rho_s d_{po}^3} \right)^{\frac{1}{2}} (R_i + R_j)^2 \left(\frac{1}{n_{po,i}} + \frac{1}{n_{po,j}} \right)^{\frac{1}{2}} \quad (5)$$

194 where R_i and R_j are radii of the sphere that circumscribes to the particles
 195 at size i and j respectively, $n_{po,i}$ and $n_{po,j}$ are the number of primary parti-
 196 cles contained in the agglomerates at size i and j , $K = 1.3807 \cdot 10^{-23}$ (J/K)
 197 is Boltzmann's constant, T is the average temperature within the combustion
 198 chamber determined with a zero dimensional three zone thermodynamics mod-
 199 els, [35], ρ_s is the density of soot, which in this case has been taken a value of
 200 1850 (kg/m³), [36] and d_{po} is the average diameter of the primary particles that
 201 make up the agglomerate, which depends on engine speed (s) and the ratio of
 202 fresh air inducted by the engine and fuel consumed (A/F), calculated according
 203 to [36].

$$d_{po}(\text{nm}) = 50.6 - 18.9 \frac{s}{2000} - 10.3 \frac{A/F}{30} \quad (6)$$

204 As it can be seen in equation (5), the number and size of primary particles
 205 and the size of the agglomerates are unknow to calculate the collision frequency.

206 Therefore, a relationship between the number of primary particles and the ag-
207 glomerate size is proposed in the following section.

208 3.3. Relationship between the agglomerate size and number of primary particles

209 Synthetic agglomerates have been generated in order to find a correlation be-
210 tween the agglomerate size and the number of primary particles. The algorithm
211 to simulate the synthetic agglomerates based on random cluster-cluster collisions
212 has been developed by the authors and further details can be found in Martos
213 *et al.* [30]. A representative example of the simulated agglomerates is shown
214 in Figure 3(b). For comparison purposes, Figure 3(a) shows a picture taken
215 with a High Resolution Transmission Electron Microscope (HR-TEM) of a real
216 particle agglomerate originated within a combustion chamber of a compression
217 ignition engine. The particle was collected using the experimental technique
218 based on the thermophoretic phenomenon reported in [36] (see further details
219 in Lapuerta *et al.* [36]).

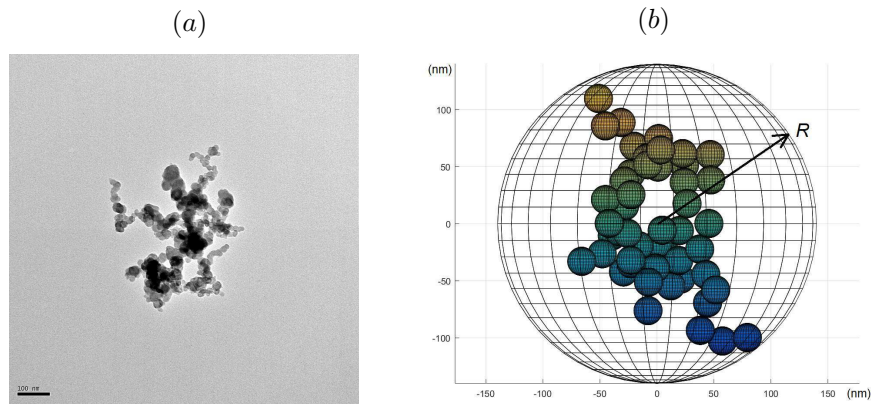


Figure 3: Views of a real agglomerate (a) and a synthetic agglomerate (b).

220 In order to find an appropriate correlation between the radius R and the
221 number of primary particles n_{po} , 250000 synthetic agglomerates were simulated
222 (gray circles) being n_{po} random. However, for the sake of clarity only 10000 sim-

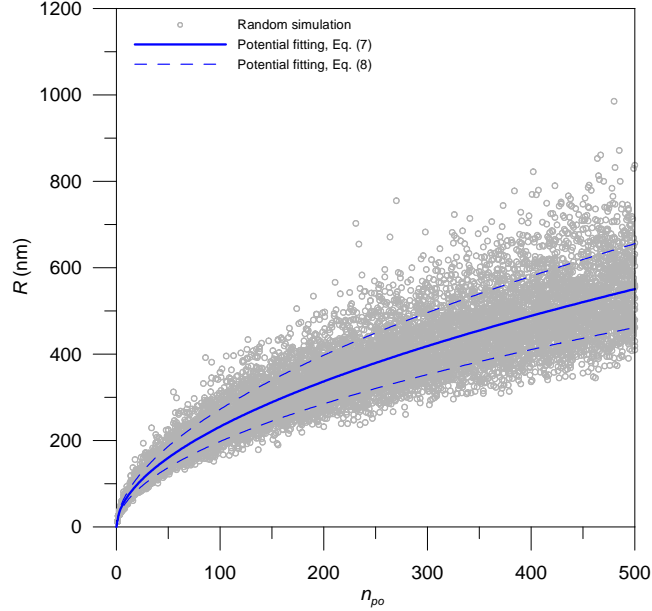


Figure 4: Random simulations (circles) and least-squares fittings (lines).

223 ulations have been plotted in Fig. 4 (one every 25 simulations). The blue solid
 224 line in Figure 4 corresponds to the potential fitting for the 250000 agglomerates,

$$\frac{\bar{R}}{d_{po}} = 0.7831 n_{po}^{0.5369}, R^2 = 0.9146, \quad (7)$$

225 being the validity of the fitting for $n_{po} \leq 500$.

226 To show that R follows a normal distribution function, the results for 500
 227 random simulations, keeping constant n_{po} for four characteristic sizes of agglom-
 228 erates, have been included in Fig. 5: small size (a) $n_{po} = 50$; intermediate sizes
 229 (b) $n_{po} = 100$ and (c) $n_{po} = 200$; large size (d) $n_{po} = 300$. Since the population
 230 for each n_{po} is higher than 50, the assumption of normality can be checked using
 231 the test of Kolmogorov-Smirnov with the correction of Lilliefors.

As can be appreciated in Fig. 5, the distribution functions follow a Gaussian
 distribution, with mean \bar{R} and standard deviation σ . Therefore, the radius of
 the synthetic agglomerate will fall into the interval $\bar{R} - \sigma < R < \bar{R} + \sigma$ with

$\sim 68.27\%$ probability. This interval is plotted in Fig. 4 with dashed-lines, being the fittings,

$$\begin{cases} \frac{\bar{R}_{+\sigma}}{d_{po}} = 0.8789 n_{po}^{0.5464}, R^2 = 0.9947, \\ \frac{\bar{R}_{-\sigma}}{d_{po}} = 0.6984 n_{po}^{0.5269}, R^2 = 0.9975. \end{cases} \quad (8)$$

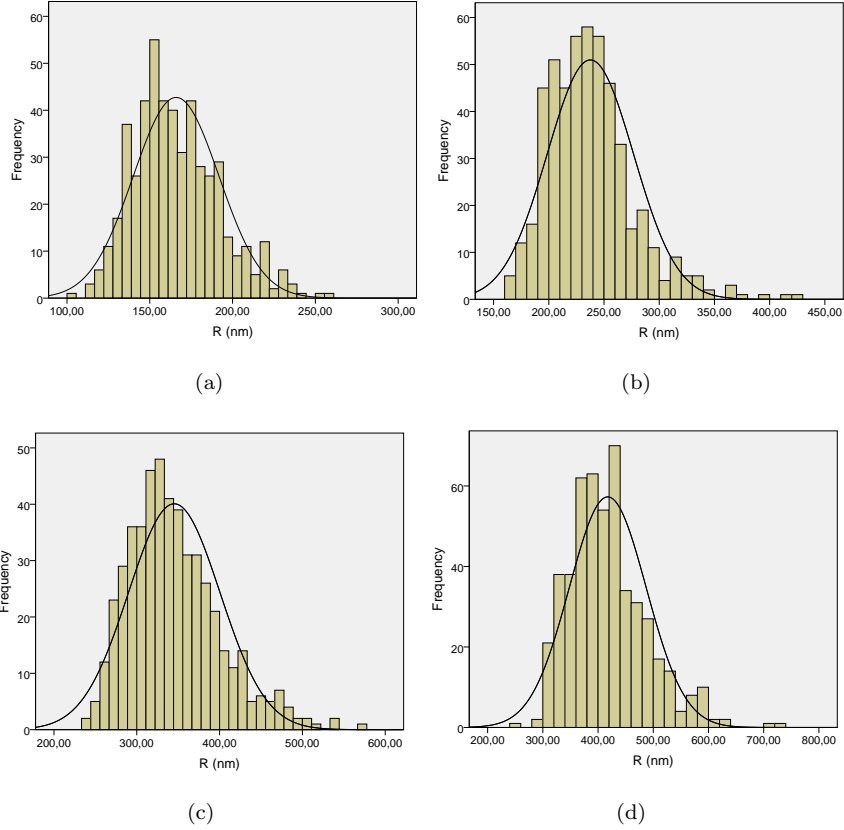


Figure 5: Number of agglomerates versus radius, keeping constant the number of primary particles that compose them. (a) $n_{po} = 50$, (b) $n_{po} = 100$, (c) $n_{po} = 200$ and (d) $n_{po} = 300$.

232 4. Results and discussion

233 Figure 6 shows the size distribution functions obtained with the model pre-
 234 sented in equation (2) (dashed red line) in which the collision radius has been
 235 determined through the adjustment proposed in equation (7) with respect to

236 the experimental size distribution function obtained with the SMPS (solid blue
 237 line). As the equivalent diameter used in the modelled distribution is different
 238 to the electric mobility diameter obtained in the experimental distribution, the
 239 diameters of electric mobility have been corrected according to the approach
 240 explained in [17]. In the y -axis, the concentration of particles for a given size
 241 has been normalized with respect to the maximum value of the particle concen-
 242 tration. Therefore, the value of the distribution function is normalized with the
 243 value of the size distribution function at his mode.

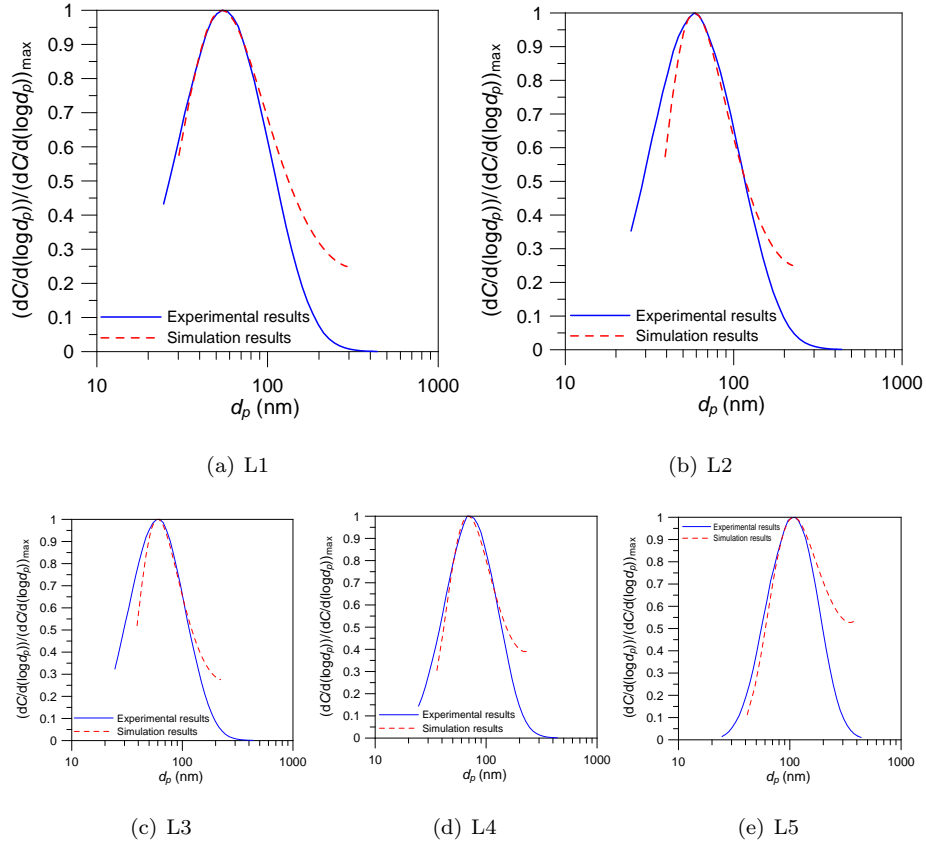


Figure 6: Size distribution functions for each operating point. (a) L1, (b) L2, (c) L3, (d) L4 and (e) L5.

244 Table 2 shows the relative error obtained when the modelled and experi-

245 mental size distribution modes are compared. The relative error obtained with
 246 the proposed semi-empirical model is lower than 3% for all tested engine op-
 247 eration modes, being lower than the uncertainty of the SMPS. The proposed
 248 model also reproduce the increase in the size distribution mode as a function
 249 of the increase in the engine load (Table 2), as well as the modelled particle
 250 size distributions are mono-modal coincident with these specific results and the
 251 majority of the experimental soot agglomerate size distributions [37]. However,
 252 as shown in figure 6, the size distribution function obtained with the proposed
 253 semi-experimental model is better suited to the experimental size distribution
 254 function for sizes less than 100 nm than for sizes larger than 100 nm.

Operating mode	d_{po} (nm)	d_{SMPS} (nm)	d_p (nm)	Relative error (%)
L1	21.36	54.25	54.71	0.85
L2	25.25	58.29	58.87	1.00
L3	26.87	62.64	61.08	2.49
L4	28.25	67.32	69.17	2.75
L5	29.26	111.40	108.96	2.19

Table 2: Modes obtained from the distribution functions for all test points.

255 It is well reported that agglomerate size distributions could be fitted to
 256 log-normal distributions [37]. Therefore, the modelled agglomerate size distri-
 257 butions are also fitted to log-normal distributions. A log-normal distribution
 258 is well defined with the mean \bar{d}_p and standard deviation σ , equation (9). The
 259 mode of the modelled distribution function will be employed as the mean of
 260 the fitted log-normal distribution, while an empirical correlation based on the
 261 SMPS results is proposed to obtain the standard deviation.

$$f(d_p) = \frac{1}{\sqrt{2\pi \ln(\sigma)}} \exp \left[-\frac{1}{2 \ln^2(\sigma)} (\ln(d_p) - \ln(\bar{d}_p))^2 \right] \quad (9)$$

262 The SMPS results have been fitted to a log-normal size distribution. The
 263 fitting has been performed minimizing the mean quadratic error between the
 264 experimental and fitting values. Figure 7 and Table 3 compare the agglomerate

265 size distribution functions, mean diameter and standard deviation for the raw
 266 (directly obtained from the SMPS), and log-fitted experimental values at all the
 267 engine operation conditions. An empirical correlation has been found between
 268 the experimental mean diameter and standard deviation obtained from the log-
 269 normal fitting (Figure 8) and equation (10). The a , b and c coefficients of
 270 equation (10) has been obtained minimizing the mean quadratic error obtaining
 271 $a = 5.183 \times 10^8$, $b = -5.497$ and $c = 1.685$, being this fitting valid when
 272 $50 \leq \bar{d}_p \leq 115$.

$$\sigma = a \bar{d}_p^b + c \quad (10)$$

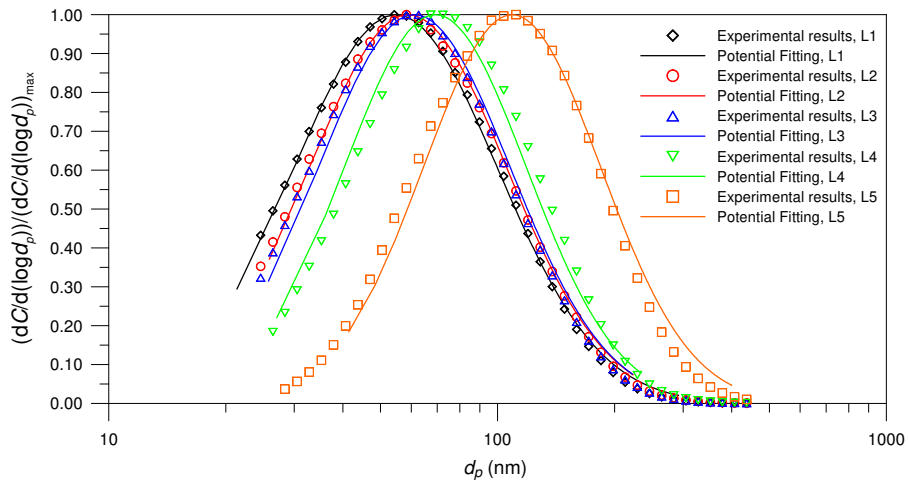


Figure 7: Comparison of agglomerate size distribution functions for all the engine operating conditions.

Operating mode	d_{SMPS} (nm)	\bar{d}_p (nm)	σ
L1	54.25	54.71	1.825
L2	58.29	58.87	1.782
L3	62.64	61.08	1.764
L4	67.32	69.17	1.725
L5	111.10	108.96	1.688

Table 3: Experimental mean diameter and experimental log-normal fitting mean diameter and standard deviation

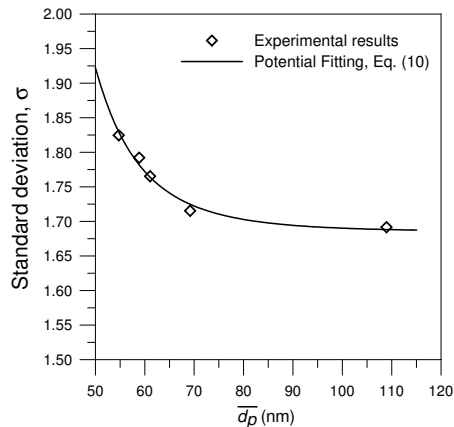


Figure 8: Empirical correlation between experimental mean diameter and standard deviation obtained from the log-normal fitting.

273 5. Conclusions

274 A semi-experimental model has been developed to obtain the agglomerate
275 size distribution function emitted by a compression ignition engine fueled with
276 standard diesel fuel. The model combines the attributes of phenomenological
277 models utilising physically motivated relations for reliable extrapolation within
278 some margins, with the computational efficiency and easiness to be handle of
279 empirical models.

280 The required inputs of the model are constants as soot density, parameters
281 as engine speed, air/fuel ratio, total volumetric soot concentration and mean
282 instantaneous in-cylinder pressure, and empirical relations to obtain primary
283 particle mean diameter and the relation between agglomerate size and number
284 of primary particles, which compose the agglomerates. An acceptable fit has
285 been obtained between the size distribution function obtained with the proposed
286 model and the experimentally measured distribution function with a Scanning
287 Mobility Particle Sizer (SMPS). The error made in the prediction of the mean
288 particle size distribution is lower than the measurement error of the SMPS for
289 all experimentally tested cases.

290 **Acknowledgment**

291 The authors express thanks to the University of Malaga for supporting
292 through a thematic network. The authors would like to thank to the gov-
293 ernment of Spain (reference PRX15/00256) for providing a research stay to F.J.
294 Martos at the University of Birmingham.

295 **Appendix A. Nomenclature**

A	air
d	diameter
C	soot concentration
D	diameter
F	fuel
i, j, k	size
L	length scale
n	number of particles
N	number of collisions
R	radius
Re	Reynolds number
s	engine speed

t	time
T	temperature
U	velocity
β	function of the collision frequency
η	Kolmogorov scale
ρ	density
ν	kinematic viscosity

296 *Subscripts*

i	index
j	index
p	particle
po	primary particle
s	soot

297 **References**

- 298 [1] V. Ramanathan, G. Carmichael, Global and regional climate changes due
 299 to black carbon, *Nature Geoscience* 1 (4) (2008) 221–227. doi:10.1038/
 300 ngeo156.
- 301 [2] A. Seaton, K. Donaldson, Nanoscience, nanotoxicology, and the need
 302 to think small, *The Lancet* 365 (9463) (2005) 923. doi:10.1016/
 303 S0140-6736(05)71061-8.
- 304 [3] 2008/692/EC, Implementing and amending Regulation (EC) No 715/2007
 305 of the European Parliament and of the Council on type-approval of motor
 306 vehicles with respect to emissions from light passenger and commercial ve-
 307 hicles (Euro 5 and Euro 6) and on access to vehicle repair and maintenance
 308 information.

- 309 [4] K. E. Lehtinen, M. R. Zachariah, Energy accumulation in nanoparticle
310 collision and coalescence processes, *Journal of Aerosol Science* 33 (2) (2002)
311 357–368. doi:10.1016/S0021-8502(01)00177-X.
- 312 [5] J.-O. Müller, D. S. Su, R. E. Jentoft, U. Wild, R. Schlögl, Diesel engine
313 exhaust emission: Oxidative behavior and microstructure of black smoke
314 soot particulate, *Environmental Science & Technology* 40 (4) (2006) 1231–
315 1236. doi:10.1021/es0512069.
- 316 [6] P. A. Bonczyk, R. J. Hall, Fractal properties of soot agglomerates, *Lang-*
317 *muir* 7 (6) (1991) 1274–1280. doi:10.1021/la00054a042.
- 318 [7] P. Meakin, Fractal aggregates, *Advances in Colloid and Interface Science*
319 28 (1987) 249–331. doi:10.1016/0001-8686(87)80016-7.
- 320 [8] C. Sorensen, The mobility of fractal aggregates: a review, *Aerosol Science &*
321 *Technology* 45 (7) (2011) 765–779. doi:10.1080/02786826.2011.560909.
- 322 [9] G. Wang, C. Sorensen, Diffusive mobility of fractal aggregates over the
323 entire Knudsen number range, *Physical Review E* 60 (3) (1999) 3036. doi:
324 10.1103/PhysRevE.60.3036.
- 325 [10] E. Knutson, K. Whitby, Aerosol classification by electric mobility: appa-
326 ratus, theory, and applications, *Journal of Aerosol Science* 6 (6) (1975)
327 443–451. doi:10.1016/0021-8502(75)90060-9.
- 328 [11] S. Z. Rezaei, F. Zhang, H. Xu, A. Ghafourian, J. M. Herreros, S. Shuai,
329 Investigation of two-stage split-injection strategies for a Dieseline fuelled
330 PPCI engine, *Fuel* 107 (2013) 299–308. doi:10.1016/j.fuel.2012.11.
331 048.
- 332 [12] M. Bogarra, J. Martin, C. H. Herreros, A. Tsolakis, A. P. York, J. Paul, In-
333 fluence of three-way catalyst on gaseous and particulate matter emissions
334 during gasoline direct injection engine cold-start. analysing emissions to

- 335 meet Euro6c legislation, Johnson Matthey's International Journal of Re-
336 search Exploring Science and Technology in Industrial Applications (2017)
337 329doi:10.1595/205651317x696315.
- 338 [13] O. Armas, A. Gómez, J. Herreros, Uncertainties in the determination of
339 particle size distributions using a mini tunnel-SMPS system during diesel
340 engine testing, *Measurement Science and Technology* 18 (7) (2007) 2121.
341 doi:10.1088/0957-0233/18/7/044.
- 342 [14] S. Park, S. Rogak, A one-dimensional model for coagulation, sintering,
343 and surface growth of aerosol agglomerates, *Aerosol Science & Technology*
344 37 (12) (2003) 947-960. doi:10.1080/027868203000899.
- 345 [15] M. Mueller, G. Blanquart, H. Pitsch, Hybrid method of moments for mod-
346 eling soot formation and growth, *Combustion and Flame* 156 (6) (2009)
347 1143-1155. doi:10.1016/j.combustflame.2009.01.025.
- 348 [16] M. E. Mueller, G. Blanquart, H. Pitsch, A joint volume-surface model of
349 soot aggregation with the method of moments, *Proceedings of the Combustion*
350 *Institute* 32 (1) (2009) 785-792. doi:10.1016/j.proci.2008.06.207.
- 351 [17] M. Lucchesi, A. Abdelgadir, A. Attili, F. Bisetti, Simulation and analysis
352 of the soot particle size distribution in a turbulent nonpremixed flame,
353 *Combustion and Flame* 178 (2017) 35-45. doi:10.1016/j.combustflame.
354 2017.01.002.
- 355 [18] N. A. Henein, Analysis of pollutant formation and control and fuel economy
356 in diesel engines, *Progress in Energy and Combustion Science* 1 (4) (1976)
357 165-207. doi:10.1016/0360-1285(76)90013-7.
- 358 [19] J. E. Dec, A conceptual model of DI diesel combustion based on laser-sheet
359 imaging, Tech. rep., SAE Technical paper (1997). doi:10.4271/970873.
- 360 [20] B. Liu, J. Hu, F. Yan, R. F. Turkson, F. Lin, A novel optimal support
361 vector machine ensemble model for NO_x emissions prediction of a diesel

- 362 engine, *Measurement* 92 (2016) 183–192. doi:10.1016/j.measurement.
363 2016.06.015.
- 364 [21] J. Asprion, O. Chinellato, L. Guzzella, A fast and accurate physics-based
365 model for the NO_x emissions of diesel engines, *Applied Energy* 103 (2013)
366 221–233. doi:10.1016/j.apenergy.2012.09.038.
- 367 [22] M. Warth, P. Obrecht, A. Bertola, K. Boulouchos, Predictive phenomeno-
368 logical CI Combustion modeling optimization on the basis of bio-inspired
369 algorithms, Tech. rep., SAE Technical Paper (2005). doi:10.4271/
370 2005-01-1119.
- 371 [23] S. Aithal, D. Upadhyay, Feasibility study of the potential use of chemistry
372 based emission predictions for real-time control of modern diesel engines,
373 *Applied Energy* 91 (1) (2012) 475–482. doi:10.1016/j.apenergy.2011.
374 10.005.
- 375 [24] C. Ericson, B. Westerberg, I. Odenbrand, R. Egnell, Characterisation and
376 model based optimization of a complete diesel engine/SCR system, Tech.
377 rep., SAE Technical Paper (2009). doi:10.4271/2009-01-0896.
- 378 [25] I. Motroniuk, R. Królak, R. Stöber, G. Fischerauer, Wireless
379 communication-based state estimation of automotive aftertreatment sys-
380 tems, *Measurement* 106 (2017) 245–250. doi:10.1016/j.measurement.
381 2016.08.004.
- 382 [26] J. Heywood, *Internal combustion engine fundamentals*, McGraw-Hill Edu-
383 cation, 1988.
- 384 [27] U. Asad, R. Kumar, X. Han, M. Zheng, Precise instrumentation of a
385 diesel single-cylinder research engine, *Measurement* 44 (7) (2011) 1261–
386 1278. doi:10.1016/j.measurement.2011.03.028.
- 387 [28] P. D. Kinney, D. Y. Pui, G. W. Mulliolland, N. P. Bryner, Use of the
388 electrostatic classification method to size 0.1 μm srm particles—a feasibil-

- 389 ity study, *Journal of Research of the National Institute of Standards and*
390 *Technology* 96 (2) (1991) 147. doi:10.6028/jres.096.006.
- 391 [29] N. A. Fuchs, *The mechanics of aerosols*, Dover Publications, 1989. doi:
392 10.1002/qj.49709138822.
- 393 [30] F. J. Martos, M. Lapuerta, J. J. Expósito, E. Sanmiguel-Rojas, Overestima-
394 tion of the fractal dimension from projections of soot agglomerates, *Powder*
395 *Technology* 311 (2017) 528–536. doi:10.1016/j.powtec.2017.02.011.
- 396 [31] S. K. Friedlander, *Smoke, Dust, and Haze: Fundamentals of Aerosol Dy-*
397 *namics*, Oxford University Press, New York, 2000.
- 398 [32] S. B. Pope, *Turbulent Flows*, Cambridge University press, 2000. doi:
399 10.1017/CB09780511840531.
- 400 [33] J. Heywood, *Combustion and its modeling in spark-ignition engines*, Inter-
401 national Symposium COMODIA 94 (1994) 1–15.
- 402 [34] J. Cai, C. Sorensen, Diffusion of fractal aggregates in the free molecular
403 regime, *Physical Review E* 50 (5) (1994) 3397. doi:10.1103/PhysRevE.
404 50.3397.
- 405 [35] M. Lapuerta, O. Armas, J. Hernández, Diagnosis of DI Diesel combus-
406 tion from in-cylinder pressure signal by estimation of mean thermodynamic
407 properties of the gas, *Applied Thermal Engineering* 19 (5) (1999) 513–529.
408 doi:10.1016/S1359-4311(98)00075-1.
- 409 [36] M. Lapuerta, F. J. Martos, J. M. Herreros, Effect of engine operating con-
410 ditions on the size of primary particles composing diesel soot agglomer-
411 ates, *Journal of Aerosol Science* 38 (4) (2007) 455–466. doi:10.1016/j.
412 *jaerosci*.2007.02.001.
- 413 [37] D. B. Kittelson, Engines and nanoparticles: a review, *Journal of Aerosol*
414 *Science* 29 (5) (1998) 575–588. doi:10.1016/S0021-8502(97)10037-4.